PERGAMON

International Journal of Heat and Mass Transfer 42 (1999) 3183–3188

International Journal of HEAT and MASS TRANSFER

Angular and transient characteristics of circular electrochemical friction probes

P.I. Geshev*, N.S. Safarova

Institute of Thermophysics, Siberian Branch, Russian Academy of Sciences, Novosibirsk, 630090, Russia

Received 30 April 1998

Abstract

Steady-state, transient and angular characteristics are calculated by finite differences for a friction probe of circular segmented shape. Diffusion in longitudinal and transversal directions is taken into account. In order to resolve accurately the infinitely high current densities at the electrode edges an oblate spheroidal system of coordinates is used. The approximate relationship for the Sherwood number Sh at $Pe > 1$ was constructed by using asymptotic and numerical results.

1. Introduction

The main aim of this work is the theoretical determination of a transient probe current $I(t)$ after electrode potential switch on. From this current the time constant of a friction probe can be obtained [1,2]. Also, as a result of the calculations a steady-state and angular characteristic of the segmented probe can be found.

Very often circular electrodes are used as friction probes. Such a type of probe is easy to fabricate by gluing a platinum wire into a supporting material. Theories for circular friction probes in a boundary layer approach for steady-state and unsteady transient characteristics are developed in Refs. [1,3]. Sobolik et al. [3] calculated, using the boundary layer approach, the angular characteristics of a three-segment circular probe. A good review of various friction probes including those of a circular shape can be found in Ref. [4].

Small probes are preferable due to their good spatial resolution and better frequency response. But for the small probe when the Peclet number is relatively small ($Pe < 1000$) the boundary layer approach fails. In this case the terms in governing equations which describe the longitudinal and lateral diffusion effects should be taken into account. The three-dimensional problem of mass transfer for circular probes have been evaluated in Refs. [5–7]. Phillips [5] presented an analytical treatment of mass transfer for a disc-shaped film at low Peclet numbers. He used the method of matched asymptotic expansions. The Green function method was used by Stone [6] for calculation of mass transfer for circular and elliptic electrodes at $10^{-3} < Pe < 10^{3}$.

At finite Peclet numbers the investigation can only be carried out numerically. This was first done by Py and Gosse [7]. In Ref. [7] a simple Cartesian coordinate system was used. But due to the infinitely large current density at the electrode edges a special ellipsoidal system of coordinates must be used for correct calculations. Only in this coordinate system can the edge effects be accurately resolved.

* Corresponding author.

0017-9310/99/$ - see front matter
PII: S0017-9310(98)00369-X

Nomenclature

c	concentration [mol m^{-1}]
c_∞	bulk concentration [mol m^{-1}]
C	dimensionless concentration c/c_∞
d	diameter of circular electrode
D	diffusivity coefficient of the control ions [m^2 s^{-1}]
E	strength of the electric field [V m^{-1}]
f	angular characteristics of circular probe
I	total electrical current [A]
I_i	single segment current [A]
j	flux density [mol m^{-2} s^{-1}]
$\bar{j}$	average mass flux on the probe [mol m^{-2} s^{-1}]
j_u	dimensionless modified mass flux density defined in (11)
Pe	Peclet number, Sd^2/D
Pe_r	Peclet number, SR^2/D
r	radial coordinate [m]
R	radius of the probe [m]
S	velocity gradient on the wall [m s^{-1}]
Sh	Sherwood number, $\bar{j}d/(Dc_\infty)$
t	time [s]
t_D	dimensionless time, $t \cdot D/R^2$
t_1	dimensionless time, $t \cdot S/Pe^{1/3}$
$\bar{t}$	dimensionless time, $\sqrt{t_1}Sh(\infty)/Sh_L$
u, v	special coordinates defined in Eq. (6)
x, y	horizontal coordinates [m]
y	vertical coordinate [m]

Greek symbols

θ	angle between flow direction and the line of cut [°]
σ, τ, φ	oblate spheroidal coordinates
ϕ	electric potential [V]

2. Oblate spheroidal system of coordinate and governing equation

The governing differential equation is

$$\frac{\partial c}{\partial t} + Sy\frac{\partial c}{\partial x} = D\Delta c \quad (y > 0). \tag{1}$$

Here

$$\Delta = \frac{\partial^2}{\partial x^2} + \frac{\partial^2}{\partial y^2} + \frac{\partial^2}{\partial z^2}$$

is the Laplace operator.

Boundary conditions are:

$$c(0,x,y,z) = c_\infty$$

$$c(t,x,y,z) = c_\infty \quad (\sqrt{x^2+y^2+z^2} \longrightarrow \infty) \tag{2}$$

$$c(t,x,y,z) = 0 \quad y = 0, \quad \sqrt{x^2+z^2} = r \le R \tag{3}$$

$$\frac{\partial c}{\partial y} = 0 \quad y = 0, \quad r > R. \tag{4}$$

The applied potential is assumed high enough so that the concentration at the electrode surface is zero. The condition (4) shows that the mass flux vanishes on the insulator surface.

Boundary conditions (2)–(4) generate an infinitely high flux density $j(\boldsymbol{x})$ at the edge of the electrode: $(x^2+z^2)^{1/2} = R$. This divergence of $j(\boldsymbol{x})$ can be obtained in an analytical form for a particular case $S = 0$. For this case the steady-state solution of the problem (1)–(4) is given by the well-known electric potential of a charged disk. This solution has an inverse square root behavior of the electric field $E = -\nabla\Phi$ at the electrode edge [1].

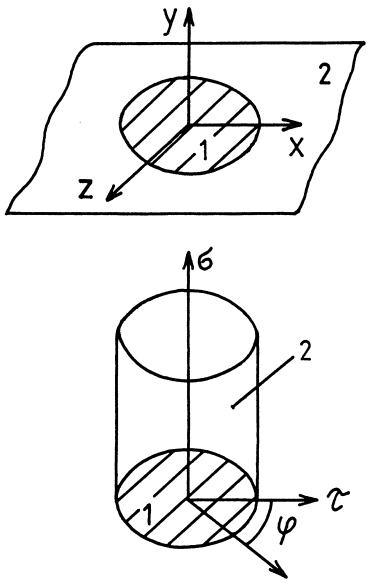

Fig. 1. System of oblate spheroidal coordinates: 1—the probe; 2—the insulator.

Accurate calculation of the solution near the edge of the electrode can be effectively performed by introducing a new oblate spheroidal coordinate system (Fig. 1) according to formula:

$$\begin{aligned} x &= R\sqrt{(1+\sigma^2)(1-\tau^2)}\ \cos\ \varphi \\ z &= R\sqrt{(1+\sigma^2)(1-\tau^2)}\ \sin\ \varphi \\ y &= R\sigma\tau. \end{aligned} \tag{5}$$

After introducing new variables

$$\sigma = \operatorname{sh} u, \quad \tau = \cos\ v \tag{6}$$

the governing Eq. (1) takes the form

$$\begin{aligned} &\frac{\partial C}{\partial t_D} + \frac{Pe}{4}\ \frac{\operatorname{sh}(2u)\ \sin\ (2v)}{4} \\ &\left\{ \frac{\cos\ \varphi}{J}\left(\frac{\operatorname{sh} u}{\operatorname{ch} u}\ \frac{\partial}{\partial u} + \frac{\cos\ v}{\sin\ v}\ \frac{\partial}{\partial v}\right)\right. \\ &\left. - \frac{\sin\ \varphi}{\operatorname{ch}^2 u \sin^2 v}\ \frac{\partial}{\partial v}\right. \\ &C = \frac{1}{J}\left\{ \frac{1}{\operatorname{ch} u}\ \frac{\partial}{\partial u}\ \operatorname{ch} u \frac{\partial}{\partial u} + \frac{1}{\sin\ v}\ \frac{\partial}{\partial v}\ \sin v \frac{\partial}{\partial v}\right. \\ &\left. + \frac{J^2}{\operatorname{ch}^2 u \sin^2 v}\ \frac{\partial^2}{\partial \varphi^2}\right\} C. \end{aligned} \tag{7}$$

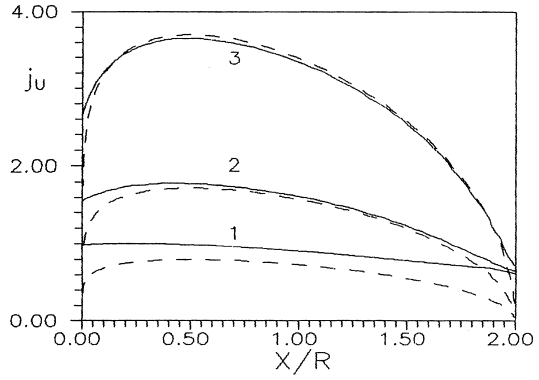

Fig. 2. Steady-state mass flux density for $z=0$: 1—$Pe=10$; 2—$Pe=10^2$; 3—$Pe=10^3$; solid line—calculated values, dashed line—boundary layer approach.

The boundary conditions (2)–(4) become

$$\begin{aligned} &C(0,u,v,\varphi) = 1, \quad C(t_D,\infty,v,\varphi) = 1 \\ &C(t_D,0,v,\varphi) = 0, \quad \left(\frac{\partial C}{\partial v}\right)_{v=\pi/2} = 0 \end{aligned} \tag{8}$$

where $J=\operatorname{sh}^2 u+\cos^2 v$ is the Jacobian of the coordinate transformation (6).

The flux density is now determined by the formula: on the electrode surface

$$\frac{\partial C}{\partial y} = \frac{1}{R\sqrt{1-(r/R)^2}}\left(\frac{\partial C}{\partial u}\right)_{u=0} \tag{9}$$

on the insulator

$$\frac{\partial C}{\partial y} = 0 \quad v = \pi/2.$$

From (9) it follows, that at the edge of the circle, where $r \to R$, the flux density has singular behavior

$$j(r) = \frac{\text{const}}{\sqrt{R^2-r^2}}. \tag{10}$$

The coordinate transformation also expands the edge region, because here $1-(r/R)^2=\tau^2$, and small steps in τ cause extremely small differences in $(R-r)$.

3. Steady-state and transient characteristics of circular probe

Eq. (7) with initial and boundary conditions (8) was solved by the method of alternating directions [8]. The calculations were done on the mesh with 200, 50, 36

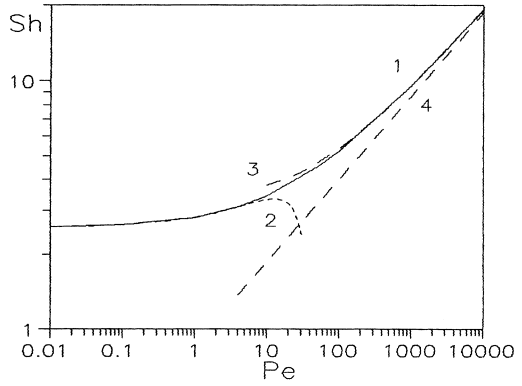

Fig. 3. Dimensionless steady-state mass transfer coefficient: 1—calculated values; 2—Phillips [5]; 3—Stone [6]; 4—boundary layer approach.

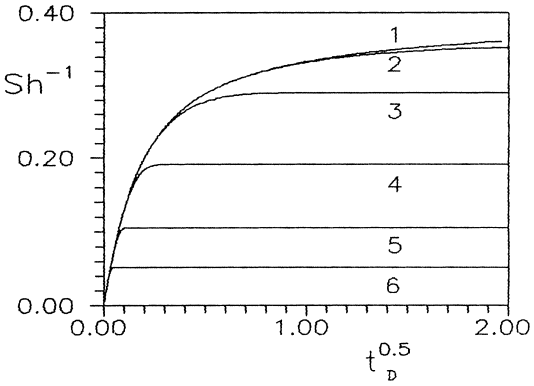

Fig. 4. Time evolution of the relative mass transfer coefficient: 1—$Pe=0$; 2—$Pe=1$; 3—$Pe=10$; 4—$Pe=10^2$; 5—$Pe=10^3$; 6—$Pe=10^4$.

(or 100, 40, 36) numbers of steps in the u-, v-, φ-directions. The sizes of the $\Delta r/R$ steps near the electrode edge were 0.00137 and 0.0007. The modified mass flux density

$$j_u = \sqrt{R^2 - r^2}\left(\frac{\partial C}{\partial y}\right)_{y=0} \tag{11}$$

for various Peclet numbers is shown in Fig. 2. As the Peclet number is decreasing the three-dimensional character of the mass transfer becomes important in the wider domain of the circular probe.

A steady-state mass transfer coefficient in a dimensionless form is the Sherwood number $Sh=\bar{j}d/(Dc_\infty)$. The complete mass transfer curve for a circular probe is shown in Fig. 3. The solid line represents numerical calculations done over the range of Peclet numbers $Pe=10^{-2}$–10^4. The short dashed line 2 represents the theoretical low Peclet number resulting from Phillips [5]:

$$Sh = \frac{2(4 - 0.11268Pe_r^{1/3})}{\pi(1 - 0.20281Pe_r^{1/3})}. \tag{12}$$

In this formula it has been taken into account that in the Sherwood and Peclet numbers [5,6] the character scale is the radius of the probe. The calculated results are remarkably accurate up to Peclet number $Pe_r < 1$. The dashed line 3 is the approximate expression proposed by Stone [6] for $Pe_r > 1$:

$$Sh = \frac{2}{\pi}(2.157Pe_r^{1/3} + 3.55Pe_r^{-1/6}). \tag{13}$$

The correlation (13) lies within 3% of the numerical results [6] for $Pe_r=10$ and within 7% at $Pe_r=5$. The dashed line 4 corresponds to the classic boundary layer solution of Leveque. At large Peclet numbers ($Pe>10^3$) obtained values of mass transfer coefficient Sh are in good agreement with the expression $Sh_L=0.866Pe^{1/3}$ and disagrees with the formula given by Py and Gosse [7] ($Sh=0.807Pe^{1/3}$). At small $Pe < 10^4$ the effects of longitudinal and lateral diffusion result in considerable deviations from the Leveque model. Calculated values of the Sherwood number can be described by approximating the formula

$$Sh = 0.866Pe^{1/3} + 3.235Pe^{-1/6} - 1.358Pe^{-1/3} + 0.0771Pe^{-2/3}. \tag{14}$$

The correlation has an accuracy better than 1% for a wide range of Peclet numbers ($1 < Pe < 10^4$).

In Fig. 4 the transient process for stepwise switching on the electrode potential is shown. The values of the relative Sherwood number obtained in the boundary layer approach [1] are expressed by approximating the formula

$$\frac{Sh(t_1)}{Sh_L} = [1 - \exp(-4.17t_1^{5/3})]^{-0.3}. \tag{15}$$

The numerically obtained mass transfer coefficients have more complex behavior and are Peclet number dependent. The numerical results for the relative Sherwood number can be represented as follows:

$$\frac{Sh(\bar{t})}{Sh(\infty)} = \frac{1 + (b_1\bar{t} + b_2\bar{t}^2)\exp(-a\bar{t}^2)}{[1 - \exp(-4.17\bar{t}^{10/3})]^{0.3}}. \tag{16}$$

Here $\bar{t} = \sqrt{t_1}Sh(\infty)/Sh_L = \sqrt{t_D}\,Pe^{1/3}\,Sh(\infty)/Sh_L$, $Sh(\infty)$—steady-state value (14). The coefficients a, b_1, b_2 obtained using the least square method are defined by

$$a = -0.0513 - 0.05428 \ln (Pe/10) + 0.03521 \ln^2 (Pe/10)$$
$$b_1 = 1.125 - 0.307 \log Pe - 0.063 \log^2 Pe \quad (17)$$
$$b_2 = -0.2403 - 0.4988 \log (Pe/10) + 0.263 \log^2 (Pe/10) - 0.0176 \log^3 (Pe/10).$$

The proposed approximation of $Sh(\bar{i})$ deviates from numerically calculated values not more than 3% for $Pe \geqslant 10$ and less than 2% for $Pe \geqslant 100$.

4. Angular characteristics for circular probe

For a double probe composed of two half-circular electrodes (Fig. 5) the angular characteristics are described by the function

$$f(\theta) = \frac{I_1(\theta)}{I_1(0)} - 1 \quad (18)$$

where $I_1(\theta)$ is an electric current from an upper electrode. This calculated numerical function is shown in Fig. 6. The theoretical results of Refs. [1] and [7] are also shown here. In Ref. [1] the angular function $f(\theta)$ was calculated in a boundary layer approach in a form

$$f(\theta) = \frac{2^{1/2}}{B(4/3,1/2)}\left[2\int_0^{\theta}(\sin\varphi \operatorname{ctg}\theta + \cos\varphi)^{2/3}\cos\varphi\,\mathrm{d}\varphi + 2^{2/3}\int_{\theta}^{\pi/2}\cos^{5/3}\varphi\mathrm{d}\varphi\right] - 1. \quad (19)$$

At large Peclet numbers ($Pe > 10^4$) the calculated values of $f(\theta)$ are in a good agreement with formula (19), the relative deviation is less than 1–2%.

For a triple probe which consists of three identical segments (Fig. 5) the angular characteristics can be described by the functions

$$f_i(\theta) = \frac{I_i(\theta)}{I_0}. \quad (20)$$

The total current of the triple probe I_0 is the sum of I_i.

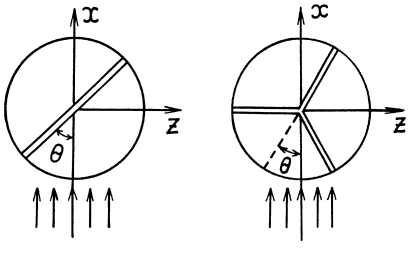

Fig. 5. Segment circular probes.

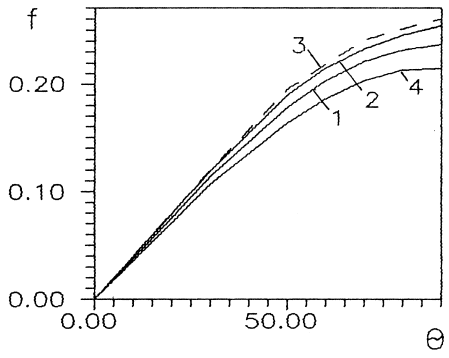

Fig. 6. Angular characteristics of twin electrode: 1—$Pe = 10^3$; 2—$Pe = 10^4$; 3—data [1]; 4—theory of Py and Gosse [7].

The current from the ith segment I_i is obtained from the expression

$$I_i = -FD\int_0^R r\,\mathrm{d}r\int_{\varphi_i}^{\varphi_{i+1}}\left(\frac{\partial c}{\partial y}\right)_{y=0}\mathrm{d}\varphi. \quad (21)$$

The calculated angular characteristic $f_i(\theta)$ is shown in Fig. 7. The values $f_i(\theta)$ obtained in the boundary layer approach and experimentally measured functions from Ref. [3] are also presented here. Some discrepancy between calculated characteristics and experimental data [3] can be explained by the nonideal geometric form of the real triple-electrode probe used in the experiments.

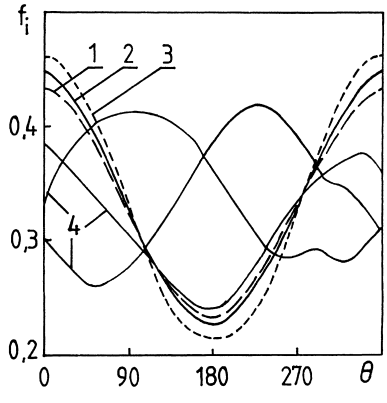

Fig. 7. Comparison of calculated and experimental angular functions: 1—$Pe = 10^3$; 2—$Pe = 10^4$; 3—boundary layer approach [3]; 4—experimental data [3].

5. Conclusion

The boundary layer approach fails near the electrode edges in the domain of several characteristic lengths $l_D = \sqrt{D/S}$. For a circular probe this peripheral ring domain occupies a relatively high part of the electrode area. Here the mass flux density is large and is proportional to an inverse square root of the distance from the edge. As a result the steady-state mass transfer at Peclet number $Pe = 10^2$–10^4 deviates considerably by 5–30% from Leveque's values.

The characteristic time needed for transient current to achieve the steady-state value for $Pe = 10^2$–10^3 is larger than the time predicted by the boundary layer theory.

For $Pe = 10^3$ the angular characteristic of the probe also deviates from its asymptotic value by 10–15%.

Acknowledgement

The authors gratefully acknowledge the financial support provided by the Russian Foundation for Basic Research, grant No. 98-03-3234.

References

[1] V.E. Nakoryakov, A.P. Burdukov, O.N. Kashinsky, P.I. Geshev, Electrodiffusion method of investigation into the local structure of turbulent flows, p. 248. Novosibirsk 1986 (in Russian).

[2] O. Wein, On the transient Leveque's problem with an application in electrochemistry, Collect. Czech. Chem. Commun. 46 (1981) 3209–3220.

[3] V. Sobolik, O. Wein, O. Gil, B. Tribollet, Three-segment electrodiffusion probes for measuring velocity fields close to a wall, Experiments in Fluids 9 (1990) 43–48.

[4] T.J. Hanratty, J.A. Campbell, Measurement of wall shear stress, in: R.G. Goldstein (Ed.), Fluid Mechanics Measurements, Hemisphere, Washington, 1983, p. 559.

[5] G.G. Phillips, Heat and mass transfer from a film into steady shear flow, Q. J. Mech. Appl. Math. 43 (1990) 135–159.

[6] H.A. Stone, Heat/mass transfer from surface films to shear flows at arbitrary Peclet numbers, Phys. Fluids A 1 (1990) 1112–1121.

[7] B. Py, J. Gosse, Sur la réalisation d'une sonde polarographique sensible á la vitesse et á la direction de l'ecoulement, C.R. Acad. Sc. Paris 269 (1969) 401–405.

[8] D. Anderson, J. Tannehill, R. Pletcher, in: Computation Fluid Mechanics and Heat Transfer, Hemisphere, New York, 1984, p. 599.